

## Effect of particle size on high purity cordierite for kiln furniture applications

E. Srinivasa Rao and P. Manohar\*

Department of Ceramic Technology, Alagappa College of Technology campus, Anna University, Chennai-600 025, India

Cordierite was synthesized using high-purity kaolin, talc, and alumina using conventional techniques for kiln-furniture application. The new raw materials subjected to magnetic separation process is to ensure total iron-free powders. The stoichiometric mixture of clay, talc, and alumina was prepared and planetary milled for several hours. The particle sizes were measured after 2, 4, 6 and 8 hours of milling respectively. The Cordierite mixtures milled at different timings were then dried at 110 °C for 24 hours. The powder blend was compacted to obtain a pellet of 12.5 mm under a uniaxial press. The pressed specimens were sent for drying and were fired at 1050, 1150, 1250, and 1350 °C. The sintered samples were subjected to X-ray diffraction (XRD). The XRD analysis indicated a clear formation of Cordierite phase for the samples sintered at 1350 °C. Scanning Electron Microscopy (SEM) studies and physical properties like bulk density, specific gravity, porosity, and water absorption were studied for the identified specimens. The hardness test using Vickers hardness tester was found to be in the range of 7.4-7.6-GPa, and the hot MOR was found to be 82-92-kg/cm<sup>2</sup>. A lower porosity for the specimens was also observed. All the results suggested that the Cordierite ceramics synthesized with the desired stoichiometry could be effectively used for kiln furniture applications.

**Key words:** Cordierite, Particle size, Hot MOR, Water absorption, Kiln furniture.

### Introduction

Cordierite ceramics are an exclusive material in ceramic technology. Cordierite ceramics have good chemical and electrical properties like high thermal resistance, low dielectric constant, low thermal expansion coefficient, and high chemical and mechanical stability, which makes it an interesting candidate for many industrial applications [1]. These properties motivate the research interest toward the synthesis of high temperature and semiconducting materials [2]. Cordierite ceramic could be used in the manufacturing of the thermal insulation materials, optoelectronic devices, plasma display panels, solar panels, catalytic convertors, multilayer circuit boards, filters, gas sensors, and kiln-furniture applications. The ternary composition (MgO: SiO<sub>2</sub>:Al<sub>2</sub>O<sub>3</sub>) of the Cordierite body molecular formulae is called as magnesium alumina silicate (Mg<sub>2</sub>Al<sub>4</sub>Si<sub>5</sub>O<sub>18</sub>) [3]. Argillaceous rock is a rare source of Cordierite mineral [4]. To prepare the Cordierite mixture, there are a few advanced and conventional methods available, such as Co-precipitation, Sol-gel, Electro spinning, and Solid state synthesis [5]. Casting, sintering, and crystallization techniques are available to achieve the Cordierite formation by the kaolin, talc alumina. The importance of the Cordierite materials is seen in the growing interest in research, and an extensive work has been carried out till date [5, 6]. The stoichiometric composition of

Cordierite ceramics is achieved by the addition of different raw materials, like silica, alumina and magnesia, clay, talc, and steatite and so on [7]. Despite the extensive research carried out on the crystallization behavior, kinetics and properties of flux-grown Cordierite ceramics by solid-state reaction, are still under study [8]. Cordierite ceramics were often used as kiln furniture due to their good thermo-mechanical properties. The isothermal sintering process of Cordierite (2MgO. 2Al<sub>2</sub>O<sub>3</sub>. 5SiO<sub>2</sub>), yields three polymorphic forms, that is α-Cordierite or indialite, β-Cordierite, and μ-Cordierite. The α-Cordierite is a stable form, with a relatively high refractoriness, low thermal expansion coefficient, and high thermal shock resistance [9, 10]. Due to these properties, Cordierite can be used in kiln-furniture and heating element support [11, 12].

The light weight Cordierite/mullite kiln-furniture materials are prepared with montmorillonite, bentonite as raw sources. The invented Cordierite/mullite kiln-furniture material has a low cost, light weight, and good energy-saving performance [13, 14]. The preparation comprises mixing of the coal gangue, aluminium hydroxide, talc, magnesite, and silica powders by stirring, molding under pressing, drying at 105-115 °C for 8-36 hours, and then heating upto 1450 °C [15]. Cordierite and Cordierite zircon ceramics are prepared, *via* sintering of the pre-ceramics, clay-mineral mixture, vermiculite, and zirconium-vermiculite, doping process without the use of long-term grinding procedures. The precursor of zircon in Cordierite was Zr-V prepared from vanadium and zirconium salt solution, via the cation exchange method [16]. Cordieritemullite (Al<sub>6</sub>Si<sub>2</sub>O<sub>13</sub>) ceramic was prepared

\*Corresponding author:

Tel : +91 44 2235 9184

Fax: +91-44-2235 2642

E-mail: pmano55@yahoo.co.in, pmano@annauniv.edu

without any cracks by generating fine mullite crystals in the solidification process. Rods or platelets (in the primary mullite phase) with less than 1- $\mu\text{m}$  diameter were generated in Cordierite formation glass during solidification and the excessive crystalline nature of Cordierite was retained [17]. Cordierite ceramics were synthesized using a composition prepared by the mixture of four different materials; talc, alumina, fly ash, and fused silica, the formation of Cordierite was achieved by solid-state sintering reactions at 1350 °C [18]. Cordierite-TiO<sub>2</sub> green ceramic was synthesized by various stoichiometric compositions of alumina, silica, and TiO<sub>2</sub>. Cordierite shows lower thermal expansion, good flexural strength, and Vickers hardness of 6.46-6.46 Gpa, was observed in samples sintered around 600-1300 °C for 3hours [19]. A composite consisting of NiCuZn ferrite and Cordierite crystallites was prepared by sintering a mixture of NiCuZn ferrite nano particles and MgO-Al<sub>2</sub>O<sub>3</sub>-SiO<sub>2</sub> glass powder [20]. The glass ceramic formation of Cordierite ternary composition doped B<sub>2</sub>O<sub>3</sub> content up to 3% was studied in the glass samples; these results were compared with those of their natural raw materials such as talc, alumina, kaolin, and boric acid [21]. Hence, the extensive importance of the Cordierite materials in ceramic industries for Kiln-furniture application has to be studied and some of the characteristics like Hot MOR studies need to be implemented.

In the present investigation, the synthesis of different particle sizes of the Cordierite ceramics by the ternary mixture (MgO: SiO<sub>2</sub>:Al<sub>2</sub>O<sub>3</sub>) was prepared by the solid-state method. These studies deal with how effectively the particle size works on hot MOR properties for Cordierite ceramics. For getting a high quality Cordierite formation, the input materials such as talc, kaolin were free-sintered before designing the composition of the Cordierite body. The Cordierite formation and crystalline nature were studied by various characterization techniques and the mechanical properties were studied. The effects of Cordierite ceramic's particle size on the sintering process are determined, where it can be used for the kiln-furniture application.

## Experimental

### Chemical

Alumina, Silicon dioxide, talc, kaolin and PVA are used as-obtained from the ABREF Pvt. Ltd, Tamilnadu, and used for synthesis and distilled water was used throughout the experimental work.

The commercial raw materials used in the preparation include talc, kaolin, and alumina. The chemical compositions of all the raw materials are shown in Table 1. The quality of raw material was very important and good quality control procedures for ensuring the chemical, mineralogical and physical characteristics of the material are essential. So the talc and kaolin were

**Table 1.** Chemical analysis of the input raw materials.

Compound	Al <sub>2</sub> O <sub>3</sub>	SiO <sub>2</sub>	MgO	Loss on ignition	Others
Talc (%)	–	60.2	33.4	5.4	1.0
Kaolin (%)	37.5	46.5	–	14.5	1.5
Alumina (%)	99	–	–	0.7	0.3

calcined at 1000 °C for eliminating unwanted materials. The theoretical composition of the overall percentage of SiO<sub>2</sub>-51%, Al<sub>2</sub>O<sub>3</sub>-35%, MgO-14% was maintained approximately in the recipe [2, 22].

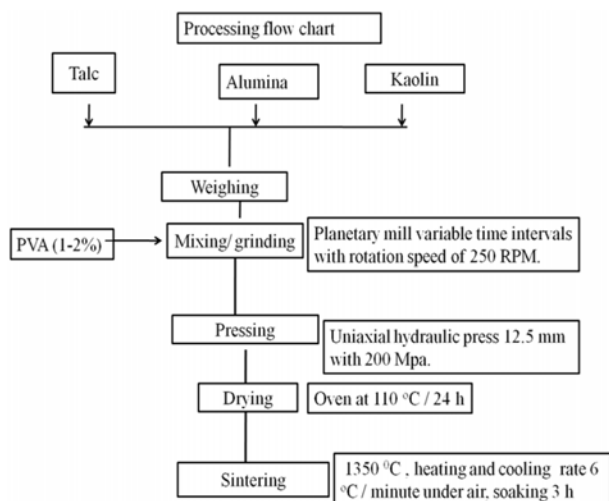
**Mixing:** The commercial raw materials were weighed and put into the planetary mill. The powder blends were dry-milled in the planetary mill (Girija engineering industries, Tamil nadu), Milling experiments were carried out using tungsten-carbide balls with a ball-to-powder ratio of (10 : 1) at rotation speeds of 250 RPM, in order to understand the planetary milling effect on the raw materials. The samples with milling hours 2, 4, 6, and 8 hours are designated with the sample code A, B, C, and D. The particle size distributions (PSDs) were determined by the Horiba particle size analyzer (Japan) for mixed and milled powder. The d<sub>50</sub> measurements for the samples A, B, C and D were obtained as 16.93  $\mu\text{m}$ , 12.72  $\mu\text{m}$ , 8.86  $\mu\text{m}$ , and 2.94  $\mu\text{m}$  respectively.

**Pressing:** The powder blend was compacted in a 10 ton capacity uniaxial hydraulic press to obtain pellets of 12.5 mm under a uniaxial press with 200MPa within one minute's time. The pressed specimens were sent for drying at 110 °C / 24 hours in an oven.

**Sintering:** The green compacts were sintered at a temperature of 1350 °C for 3hour's soaking time in the tungsten-carbide electrode furnace (box furnace from VB Ceramics); the heating rate was maintained at 6 °C/minute under air.

### Physico-chemical characterization techniques

The phase composition of raw materials and sintered bodies was performed by the X-ray diffraction technique (Rigaku Mini flexIIc) with Cu K $\alpha$  (1.54) radiation in the 2 $\theta$  range of 5-70 °. ICDD powder-diffraction files were utilized for the identification of the crystal phases. The physical properties of all the sintered bodies, such as bulk density, porosity, and water absorption were measured by the Archimedes method. The hardness of the samples was measured using Vickers hardness test (Zwick). Hot MOR were carried out by the process of making the bars by LBH values (151  $\times$  25  $\times$  25 mm) and placed inside the kiln and test was carried out at 1250 °C to determine the strength at working temperature. The test was conducted at high temperature Hot MOR furnace from VB Ceramics, India. The Field Emission Scanning Electron Microscope (FESEM) analysis was carried out on a FESEM-SUPRA 55-CARL ZEISS SEM for the sintered specimens of Cordierite A, B, C, and D. The particle-size



distribution of the Cordierite recipe in water was analyzed with the HORIBA Laser Scattering Particle Size Distribution Analyzer LA-950.

### Synthesis of the Cordierite body.

The Cordierite body preparation method was followed by a solid-state synthesis method and all the different recipes followed the same flow chart except grinding time. The preparation method of the specimens is given as a flow chart below.

## Results and Discussion

### Chemical analysis

The chemical composition of raw materials ( $\text{SiO}_2$ ;  $\text{Al}_2\text{O}_3$ ;  $\text{MgO}$ ) was analyzed by the gravimetric analysis method and given in Table 1. The Cordierites A, B, C, and D have a loss on ignition of around 0.7-14.5%, and on ignition the magnetite specimen gets decreased upon increasing the percentage of alumina. It is due to the formation of the Cordierite body as can be seen from the XRD.

### FESEM analysis

The FESEM analyses of the sintered ceramic specimens are shown in Fig. 1, to know the formation of Cordierite by the ternary mixture. The homogeneity, surface morphology, and porosity of the samples can be illustrated from the microscopic analysis. The microscopic images of the A, B, C, and D samples show a regular homogenous distribution of the Cordierite. The Cordierite ceramics A-D did not observe any crack or wipe of the samples, when they were sintered/annealed at 1350 °C. From Fig. 1, most of the particles are seen to be spherical in shape and particles are not of the same size; the samples A and B have an opaque nature, but the variation in the porosity and size of the particles is clearly seen in the samples C and D. In the higher magnification of the FESEM images, the particle size of each sample was calculated to be around 10  $\mu\text{m}$ . This

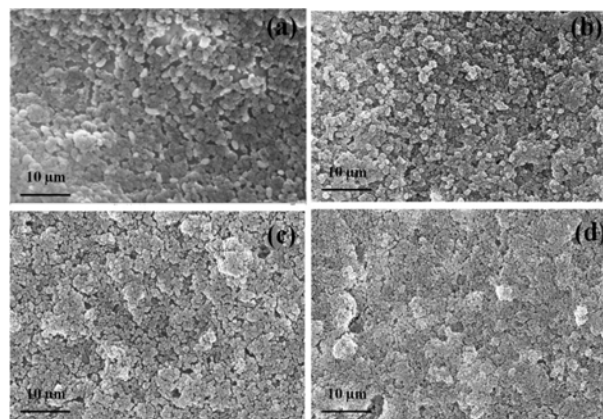
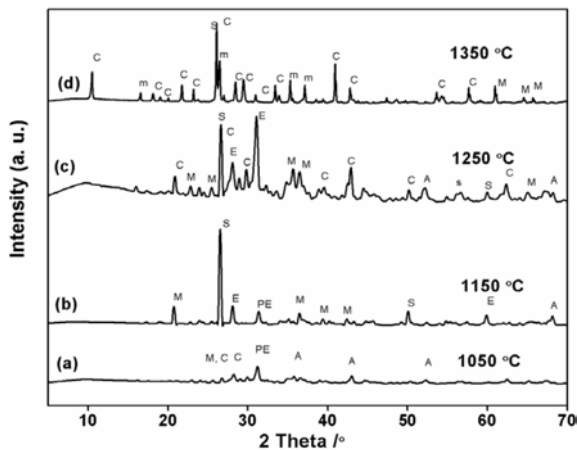


Fig. 1. FESEM analysis of the samples A, B, C, and D.

image clearly shows the brightness of samples, improving A-D; it suggests that while sintering the sample, the crystallization of the sample occurs for the Cordierite samples. The mean particle size also shows the same phenomenon for the samples, when samples' particle sizes were determined by the wet method. From Fig. 1(D), the particles' greater compaction can be observed in sample D, when compared to the C, B, and A specimens. During the formation of Cordierite phase, alumina particles in the sub-micrometer range and the bright spots are clearly visible from the micro images; it suggests that the fine powder of the alumina along with the kaolin and silica segregation was no longer observed. During the sintering process, Cordierite can be transformed into different phases, and a few free alumina fine particles and mullite can be obtained. The phase transformation analyses can be revealed from the XRD analysis. The SEM and XRD analyses suggest the same [23, 24]. A microscopic analysis clearly evidences the formation of the compactness of specimens with different particle sizes during the sintering process.

### X-ray diffraction studies

The XRD patterns of Cordierite D were revealed at 1050, 1150, 1250, 1350 °C and provided in Fig. 2. Figure 2 (1250 & 1350 °C curves) clearly suggests the Cordierite phase (PDF#48-1600) after treatment of the sample up to 1350 °C. On heating the sample up to 1150 °C, the XRD pattern shows the formation of the enstatite phase. The crystallization of the Cordierite phase increased in the range of 1350 °C. Fig. 2 indicates that the present solid-state reaction has undergone a phase change at various sintering temperatures. In the XRD patterns at 1050 °C, the crystalline nature of the sample's less intensity and peak is observed in the 2 theta values 20°, 28°, 31°, 36°, and a moderate intensity peak at 26° was observed (JCPDS card no:87-1487,79-1457 and 86-1629). The moderate intensity peak at 26° may be due to the formation of mullite. On further heating of the sample from 1000 °C to 1150 °C, changes in the phase were observed due to the  $\mu$ -Cordierite phase (JCPDS card



**Fig. 2.** The XRD patterns of the Cordierite specimen D at (a) 1050 °C, (b) 1150 °C, (c) 1250 °C and (d) 1350 °C, the corresponding phases also indicated as A: Alumina, E: Enstatite, C: Cordierite, PE: Proto-enstatite, M: Mullite, and S: Silica.

no:79-1457,48-1600,11-0273), and here, small peaks were observed due to the spinel formation ( $\text{MgAl}_2\text{O}_4$ ) on the Cordierite body [12, 25].

At the sintered temperature of 1250 °C, the formation of a mullite phase along with negligible amounts of enstatite, forsterite was observed. It is clearly shown in Fig. 2 that variable phases are formed at different temperatures, the major peaks initially were absorbed by enstatite, free alumina, and silica. When the temperature goes higher, all these individual alumina, silica, proto-enstatite, forsterite, and mullite peaks get reduced and converted to form Cordierite. More or less impurities were no longer observed in the final phase formation. The new peaks were observed at 1350 °C, where as this peak disappeared in the other three cases. The new peaks at 2 theta values of 10.4°, 21.5°, 23.2°, 28.7°, 30.7°, 37.3°, 40.7°, 42.7°, 53.2° are confirmed as  $\alpha$ -Cordierite phases of the Cordierite specimen. Another negligible peak is also found due to the formation of mullite, and here, the  $\mu$ -Cordierite phase was no longer observed. Hence, the crystallizations of Cordierite-phase formation are clearly seen in the spectra. The obtained Cordierite peaks are well matched with those of the earlier investigation [26]. Based on the variable densities of phases, different peaks were observed in the obtained XRD pattern, like Cordierite phase ( $2.499 \text{ g/cm}^3$ ) which has a low density when compared with that of alumina ( $3.987 \text{ g/cm}^3$ ) and enstatite ( $3.28$ ) [27]. As it worked in XRD for the D sample with different temperatures, it is observed that all the other Cordierites might show similar behavior of the formation of Cordierite phases. The microscopic analysis also confirms the same. The comparison of the XRD and FESEM analysis of the Cordierite shows well ordered and formed crystalline phases.

### Particle size distribution (PSD) curves

The granulometric distribution of the milled mixture

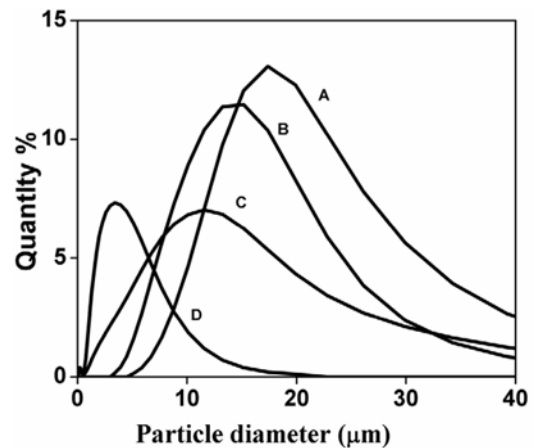


**Fig. 3.** The particle size distribution curves of the samples A, B, C, and D.

was obtained from the particle size analyzer by the Horiba particle-size analyzer and reproduced in Figs.3 and 4. For the diameter at 10%, the particle size was 5  $\mu\text{m}$ , for the diameter at 50%, the particle size was below 10  $\mu\text{m}$  and for the diameter at 80%, the particle size was at 20  $\mu\text{m}$ . The mean diameter *approx.*  $D_{50}$  of the Cordierite recipe were calculated as 16.93  $\mu\text{m}$ , 12.72  $\mu\text{m}$ , 8.86  $\mu\text{m}$ , and 2.94  $\mu\text{m}$  as A, B, C, and D respectively by the PSD width. The PSD curves are shown in Fig 3, slightly moving from a higher particle size (16.93  $\mu\text{m}$ ) to a lower particle size (2.94  $\mu\text{m}$ ) based on increasing the grinding time. In Figs 3 and 4, no bi-model curves were observed; but in Fig. 3, the samples A and B are seen little uneven, as with increase in the grinding time, the curve clearly indicates uniformity in recipe that is shown in samples C and D. The decrease in the particle size from 16.93 to 2.94  $\mu\text{m}$ , was seen for A-D sintered Cordierite. The D sample has a lower particle size; it may be effectively used for even packing of crystals and formation of the lower porosity body. Hence, the sintering behavior and milling of the sample with variable time intervals can alter the particle size of the Cordierite body [28-30]. The PSD studies can be compared with the microscopic analysis; these studies reveal the same and the particle size effect on kiln furniture behavior and water-absorption capacity.

### Hot MOR studies

The flexural strength of the sintered Cordierite A, B,

**Table 2.** Physical properties of the Cordierite specimens.

Sample	PSD ( $\mu\text{m}$ )	Bulk density (g/cc)	Porosity %	Water absorption %	True sp.gr. (g/cc)
A	16.93	1.95	32	15.52	2.41
B	12.72	2.1	26	13.5	2.45
C	8.86	2.33	21	10.23	2.52
D	2.94	2.45	12	6	2.60

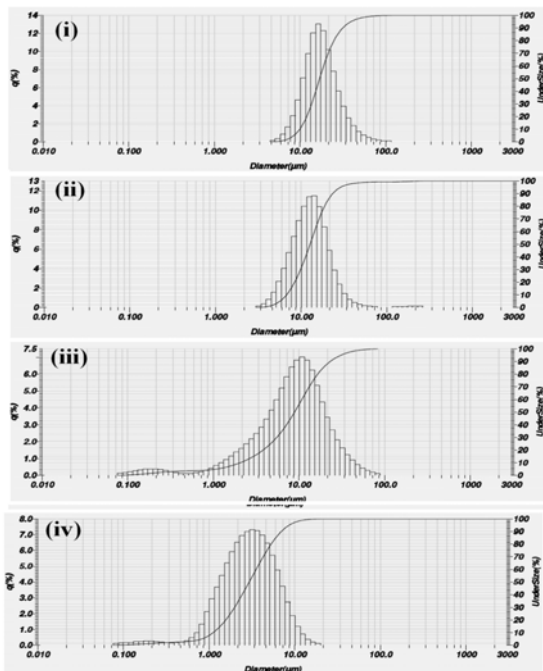


Fig. 4. The particle-size distribution curves (bar diagram) of the samples (i) A, (ii) B, (iii) C, and (iv) D.

C, and D was measured by the Hot MOR testing equipment (V B Ceramics consultants, Tamil nadu). The bending strength of A, B, C, and D was calculated by using the relation.

$$\text{MOR} = \frac{3PL}{2BD^2} \quad (1)$$

Where, P = Load applied, L = Length of the supports, B = Breadth of the specimen, and D = Thickness of the specimen.

From equation 1 the Cordierite specimen was found to have the MOR as 82, 84, 88, and 94-kg/cm<sup>2</sup> for A, B, C, and D respectively. From Table 2, the particle sizes of the A, B, C, and D values were in decreasing order, whereas the bending strength of the Cordierite is increased. Here, it was observed that A, and B exhibit a comparable flexural strength while the flexural strength of D is higher when compared to that of A, B, and C, due to the formation of good crystallinity of the Cordierite body, which enhances its compatibility. The Hot MOR studies reveals sample D as having good flexural strength at 2.94 µm [29].

#### Hardness test

The hardness of the Cordierite body of A, B, C, and D was tested by the Vickers method using equation [18], and shown in Fig. 5.

$$\text{HV} = 1.854F/d^2$$

the hardness was found to be 7.4, 7.5, 7.6, and 7.8 GPa for the A, B, C, and D specimens [19]. It is observed

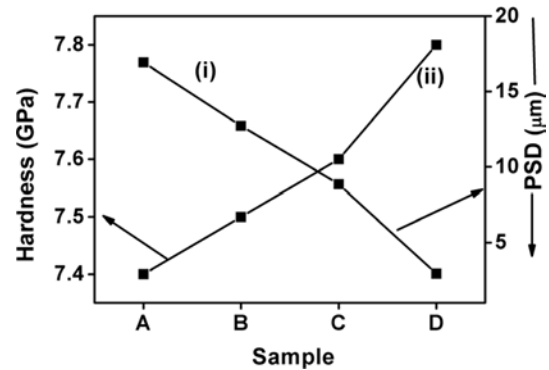


Fig. 5. Graph of the PSD and hardness sample A, B, C, and D.

that the hardness of sample D is higher than that of the other Cordierite specimens; it may be that the lower particle size influences the good packing and well-sintered Cordierite formation.

#### Physical properties of the Cordierite specimens

The density, porosity, and water absorption of the Cordierite bodies of A, B, C, and D were evaluated by the Archimedes principle and the measurements are given in the Table 2.

From Table 2, the bulk density, porosity, and water absorption of A, B, C, and D are decreased along with particle-size reduction. The test of specific gravity measured was carried out by the specific gravity bottle method using equation 2.

$$\text{True specific Gravity} = \frac{(M_2 - M_1)\rho_0}{(X - Y)} \quad (2)$$

where,  $M_1$  = weight of the bottle,  $M_2$  = weight of the bottle + solid,  $M_3$  = weight of the bottle + solid + water,  $M_4$  = weight of the bottle + water, and  $\rho_0$  = density of water,  $X = M_4 - M_3$ ,  $Y = M_3 - M_2$

From Table 2, the true specific gravity values are found to be 2.41, 2.45, 2.52, and 2.6-Kg/m<sup>3</sup> for A, B, C, and D because of good crystalline formation of the Cordierite phase, and the specific gravity confirms the Cordierite body [18, 31-34].

#### Conclusions

The Cordierite body was synthesized by a ternary mixture of MgO-Al<sub>2</sub>O<sub>3</sub>-SiO<sub>2</sub> powder by the solid state synthesis method. The mixture was milled for 2, 4, 6, and 8 hours respectively, to achieve different sizes of Cordierite specimens. One of the Cordierite specimens (D) was sintered at various temperatures and then studied by the powder XRD to know the different phases of Cordierite body sample, and thus, it was inferred that the formation of the Cordierite body with good crystalline nature was at 1350 °C. The crystallization of Cordierite phase was studied in the range of 1050-1350 °C. From XRD, the other phases like mullite, enstatite, proto-enstatite also were observed at lower temperatures. The FESEM analysis

clearly indicates the formation of various sized specimens, particle compactness, and well phase formation during the sintering process of the Cordierite body. The PSD curves also suggest that the average size of the particles is decreased in the milling process on increasing the grinding time. The physical properties were also measured by the Archimedes principle, and water absorption was more for the larger particle-sized specimens, porosity decreased along with the lower particle sizes, and increased the true specific gravity. The hardness of the sample was found to be 7.8 GPa for sample D; it can compare with the theoretical Cordierite body. The Hot MOR studies clearly suggest that the Cordierite specimens exhibited excellent strength at working temperature. Hence, the high purity Cordierite samples with less particle size can be effectively used in the kiln-furniture applications with more life cycles.

### Acknowledgments

The authors gratefully acknowledge the financial support received from the Department of Science and Technology by sanctioning the project to Dr.P.Manohar (DST/TSG/Ceramic/2011/134-G. 14.08.2012).

### References

1. C. Shu, X. Mingxia, Z. Cailou and T. Jiaqi, *Mater. Res. Bul.*, 37 (2002) 1333-1340.
2. J.B.R. Neto and R. Moreno, *Appl. Clay Sci.*, 38 (2008) 209-218.
3. M.N. Khezrabadi, R. Naghizadeh, P. Assadollahpour and S.H. Mirhosseini, *J. Ceram. Process. Res.*, 8 (2007) 431-434
4. D. A. Deer, R. A Howie, and J. Zussman, *J. Eur. Ceramic Soc.*, 21 (2001) 185-193.
5. S. Mei, J. Yang and J.M.F Ferreira, *J. Eur. Ceram.Soc.*, 21 (2001) 185-193.
6. W. Winter, *J. Mater. Sci.*, 32 (1997) 1649-1655.
7. Y.N. Shieh, R.D. Rawlings and R.F. West, *Mater. Sci. Technol.* 11 (1995) 863-869.
8. S. Kurama and H. Kurama, *Ceram. Inter.*, 34 (2008) 269-272.
9. P. Predecki, J. Haas, J. Faber and J.L. Hitterman, *J. Am. Ceram. Soc.*, (1987) 175-182.
10. V.K. Marghussian, U. Balazadegan and B. Eftekhari-yekta, *J. Eur. Ceram. Soc.*, 29 (2009) 39-46.
11. C.Ghitulica, E.Andronesco, O. Nicola, A. Dicea and M. Birsan, *J. Eur. Ceram. Soc.*, 27 (2007) 711-713.
12. M.A. Camerucci, G. Urretavizcaya and A.L. Cavalieri, *Ceram. Int.*, 29 (2003) 159-168.
13. X. Xiayun, G. Haizhu, Q. Yuliang, K. Min, W. Jianzhong and Y. Jinming., *From Faming Zhuanli Shenqing* (2014), CN 103524123 A 20140122.
14. S.Rattanavadi, L.Punsukumtana, N. Thavarungkul and N. Srisukhumbowornchai, *J. Aust. Ceram. Soc.*, 50 (2014) 118-125.
15. Y. Wen, L. Nan, K. Changming, W. Yaowu, H. Bingqiang, Y. Guilin and L. Yousheng., *Faming ZhuanliShenqing.*, (2012), CN 102557717 A 20120711.
16. M. Valaskova, S. Martynkova, G.J. Zdralkova, J. Vlcek and P. Matejkova., *Mater. Lett.* 80 (2012) 158-161.
17. U. Shunkichi, T. Yasuhiro and N. Zenbe, *J. Ceram. Soc. Jpn.*, 111 (2003) 528-532.
18. R. Goren, C. Ozur and H. Gomez, *Ceram. Int.*, 6 (2006) 53-56.
19. S.K. Marikkannan and E.P. Ayyasamy, *J. Mater. Res. Tech.*, 2 (2013) 269-275
20. Z.Yue, L. Li, J. Zhou, H. Zhang, Z. Ma and Z. Gui, *Mater. Let.*, 44 (2000) 279-283.
21. Y. Demirci and E. Gunay, *J. Ceram. Process. Res.* 12 (2011) 352-356.
22. D.W. Richerson. *Modern ceramics engineering* 3<sup>rd</sup> ed., Informa Taylor and Francis, New York, 2006.
23. E. Gunay, *J. Ceram. Process. Res.*, 11 (2010), 591-597.
24. Z. Acimovic, L. Pavlovic, L. Trumbulovic, L. Andric and M. Stamatovic., *Mater. Lett.*, 57 (2003) 2651-2656.
25. Y. Kobayashi, K. Sumi and E.Kato, *Ceram. Int.*, 26 (2000) 739.
26. B.P. Saha, R. Johnson, I. Ganesh, G.V.N. Rao, S. Bhattacharjee, Y.R. Mahajan, *Mater. Chem. Phy.*, 67 (2001) 140-145.
27. E.M.M. Ewais, Y.M.Z. Ahmed and A.M.M. Ameen, *J. Ceram. Process. Res.*, 10 (2009) 721-728.
28. F.A.C. Oliveira and J.C. Fernandes, *Ceram. Int.*, 28 (2002) 79-91.
29. H.S. Tripathi and Banerjee G., *Ceram. Int.*, 25 (1999) 19-25.
30. E.Yalamac and S. Akkurt, *Ceram. Int.*, 32 (2006) 825-832.
31. W. Ryan and C.Radford, *Whitewares: Production, Testing, and Quality Control*, Pergamon press, (1987).
32. F. A.C. Oliveira, N. Shohoji, J.C. Fernandes and L.G. Rosa, *Sol. Energy*, 78 (2005) 351-361.
33. B. Tang, Y.W. Fang, S.R. Zhang, H.Y. Ning and C.Y. Jing, *Ind. J. Eng.Mater. Sci.* 18 (2011) 221-226.
34. A. Yamuna, R. Johnson, Y.R. Mahajan and M. Lalithambika, *J. Eur. Ceram. Soc.*, 24 (2004) 65-73.